Construction and Building Materials 301 (2021) 124242

Contents lists available at ScienceDirect

Construction and Building Materials

journal homepage: www.elsevier.com/locate/conbuildmat

Effect of high temperature on the mechanical properties of concrete reinforced with different fiber contents

Ronney R. Agra [a,b,*], Ramoel Serafini [a,b], Antonio D. de Figueiredo [a]

[a] Department of Civil Construction Engineering, Polytechnic School of the University of São Paulo | Avenida Professor Almeida Prado, Travessa 2, 83, 05424-970 São Paulo, Brazil
[b] Institute of Technological Research | Avenida Professor Almeida Prado, 532, 05508-901 São Paulo, Brazil

ARTICLE INFO

Keywords:
Steel fiber reinforced concrete
Double edge wedge splitting test
Elevated temperature
Post-crack behavior
Compressive behavior

ABSTRACT

This study evaluates the effect of fiber content on the thermo-mechanical properties of steel fiber reinforced concretes (SFRC) and contributes to the definition of design-oriented parameters for SFRC after temperature exposure, which are limited in literature and current guidelines. The mechanical behavior of samples subjected to high temperatures (25 °C ≤ T ≤ 750 °C) and produced varying the fiber contents were analyzed. The tensile properties were determined using the Double Edge Wedge Splitting (DEWS) test, which proved to be a viable methodology to evaluate the post-crack behavior of SFRC exposed to high temperatures. The rate of degradation in compressive and tensile strength was reduced for higher contents of steel fibers after exposure to elevated temperatures. The reductions in compressive strength and the elastic modulus were more severe than those prescribed by European guidelines. Additionally, the tensile properties reduced significantly for T ≥ 450 °C. Also, a temperature-related reduction rate in the post-crack tensile properties was parameterized for all the fiber content samples, in which only 20% of f_{Fts} and 30% of f_{Ftu} room temperature values were retained after exposure to 600 °C, which are higher values comparing the European guidelines.

1. Introduction

Steel fiber reinforced concrete (SFRC) have been increasingly employed in civil engineering applications, especially due to its technical and economic benefits. The publication of the *fib* Model Code-10 [1] was an important milestone to promote the use of FRC for structural purposes [2,3]. However, the standards do not present an adequate approach for the design of SFRC structures under fire [4,5]. Although recent studies analyze the influence of the temperature on composites [6–15], the aforementioned lack of parameters reveals the need for investigations regarding the mechanical behavior of the SFRC when exposed to high temperatures, in order to characterize the tensile strength of the matrix (f_{Ft}), the post-crack tensile strength related to serviceability (f_{Fts}), and the the post-crack tensile strength at ultimate limit state (f_{Ftu}) [1]. It is possible to estimate the gradient degradation provided by the fire inside the SFRC by determining the temperature-related mechanical properties and obtaining the internal temperature distribution in the composite [16–18]. Accordingly, the temperature-related mechanical properties can serve as a basis for numerical models aimed at defining safety parameters applied to SFRC structures exposed to fire [19].

Several methodologies have been proposed to determine the post-crack tensile properties of SFRC at room temperature, however these methodologies have limitations when applied to specimens exposed to elevated temperature [17,20–24]. Bending tests are commonly employed to determine the tensile properties of SFRC after exposure to elevated temperatures [20,21] and even after exposure to fire [17]. However, the considerable size of the specimen, the fragility of the samples after heating and the increase in plastic deformations located in the contact region between the roller and the specimen may lead to distortions of the bending test results. Moreover, the compressive region generated in bending test have a significant contribution to the maximum flexural moment, which induces an increase in post-crack tensile strength [1]. The different compressive and tensile degradation coefficients may induce an even more considerable difference between f_{R3} and f_{Ftu} after exposure to elevated temperature, which may make the conversion of the Rigid-Plastic model (*i.e.* $f_{R3}/3$) to be inadequate. The aforementioned discussion are still open topics that still require further investigation in order to define an adequate approach to determining the post-crack tensile parameters of SFRC after temperature exposure.

* Corresponding author.
E-mail address: ronney.agra@usp.br (R.R. Agra).

https://doi.org/10.1016/j.conbuildmat.2021.124242
Received 3 December 2020; Received in revised form 12 June 2021; Accepted 12 July 2021
Available online 27 July 2021

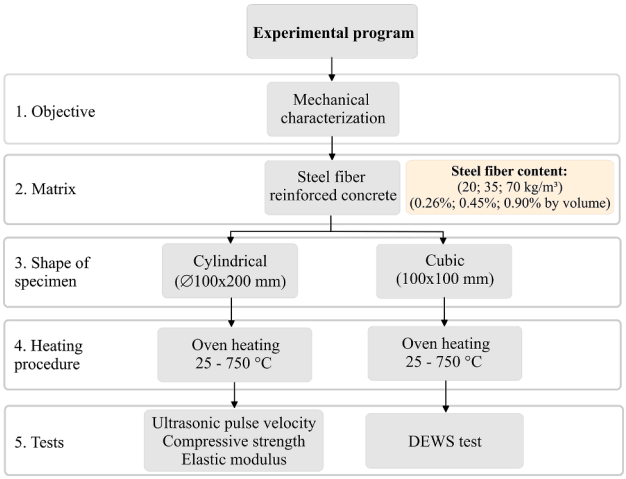

Fig. 1. Scheme adopted for the experimental program of this study.

Table 1
Dosage of materials to produce 1 m^3 of each SRFC composition.

	SFRC-0.26	SFRC-0.45	SFRC-0.90
Materials	Dosage (kg/m^3)	Dosage (kg/m^3)	Dosage (kg/m^3)
Portland cement	400	400	400
Silica fume	22	22	22
Siliceous river sand	403	403	403
Artificial granite sand	269	269	269
Coarse granite aggregate d_{max}:	330	330	330
9.5 mm	770	770	770
Coarse granite aggregate d_{max}:	165	165	165
19 mm	2.6	3	4.1
Water	0.8	0.8	0.8
Superplasticizer	20	35	70
Synthetic micro-fiber			
Hooked-end steel fiber			

Table 2
Results of d_{10}, d_{50}, d_{90} and fineness modulus for the aggregates.

Materials	d_{10} (μm)	d_{50} (μm)	d_{90} (μm)	FM
River sand	177.79	341.13	705.66	1.15
Artificial sand	69.03	2580	4230	3.55
Aggregate $d_{máx}$:9.5 mm	2390	5540	8720	5.45
Aggregate $d_{máx}$:19 mm	9210	14,390	18,280	6.80

Some indirect tests for determining post-crack properties have been investigated [22–24]. Rambo et al. [24] investigated the applicability of the Double Punch test (DPT) to determine the post-crack tensile properties of macro-synthetic fiber reinforced concrete (MSFRC) exposed up to 600 °C. The results in terms of f_{Ftu} were inconclusive for specimens exposed to high temperatures, which was attributed to the additional frictional interaction between the deteriorated matrix and the piston. Serafini et al. [25] demonstrated that the Double Edge Wedge Splitting (DEWS) test [26] can be a suitable alternative for the determination of f_{Ftu} after exposure to elevated temperatures. The aforementioned study [25] had limited the experimental program to a single fiber content and the applicability of the test remains uncertain for higher fiber contents. Thus, the evaluation of the post-crack tensile strength of SFRC using the DEWS test [26] is not sufficiently explored in the literature, especially for concretes with strain-hardening behavior in post-temperature conditions. In this context, the present study aims to evaluate the effect of the temperature on the mechanical properties of SFRC with steel fiber contents of 0.26%, 0.45%, and 0.90% in volume.

A lack of studies focused on evaluating the applicability of the DEWS test for concretes exposed to elevated temperatures is verified, especially considering SFRC with a strain-hardening behavior. Therefore, the current dosages have focused on evaluating fiber reinforced concretes with fiber content lower than the critical fiber volume (e.g. 0.26% and 0.45%) and at the theoretical critical fiber volume (0.90%) [27]. The investigation of SFRC with fiber content lower than the critical volume is relevant since it is commonly employed for economic and technical purposes in infrastructure systems, such as tunnels [28].

The results obtained seek to establish behavior parameters of the SFRC exposed to elevated temperatures and contribute to minimize the lack of reliable technical data related to the theme. The evaluation of the post-crack tensile strength of SFRC was performed using the DEWS test [26]. Although this test method is relatively new, its use in this study presents promising results in determining the tensile properties of SFRC, either with softening or hardening behavior. Therefore, the DEWS test is a possible alternative for establishing constitutive equations and for evaluating structural safety, in accordance with *fib* MC-10 [1], especially because it induces a mode I fracture in the SFRC. Furthermore, the DEWS test may be a suitable test method to be implemented in future studies and guidelines worldwide.

2. Experimental program

Fig. 1 presents the scheme adopted for the experimental program of this study. Mechanical tests were performed to assess the composite behavior before and after temperature exposure. The SFRC was evaluated with respect to the post-crack tensile strength through the DEWS test, while the compressive strength and elastic modulus were also determined by means of compressive strength tests. These evaluations provide conditions to assess the influence of temperature on the behavior of the composite. This paper is part of a larger research project that aims to evaluate the effect of elevated temperatures on SFRC structures. Therefore, a detailed description of the materials can be found in Serafini et al. [17]. For the convenience of the reader, a brief description of the materials used in this research is provided.

2.1. Materials

A type I Portland cement (CEM I 52.5R) and silica fume type Elkem 920-U with 98% SiO_2 were employed as cementitious materials in this study. The particle packing was promoted using artificial (d_{max}: 4.8 mm) and river sand (d_{max}: 2 mm) as fine aggregates and two coarse granite aggregates (d_{max}:19 mm and d_{max}:9.5 mm). A polycarboxylate-based superplasticizer, GCP ADVA Cast 525, was used to provide consistency to the mix. The concrete matrix was reinforced with cold-drawn, hooked-end steel fibers, Dramix 3D 80/60-BG. Polypropylene micro-fibers, from the Brazilian company Neomatex, were also employed in the mixture. The use of micro-fibers (length = 12 mm and diameter = 0.03 mm) has a negligible influence in the post-crack tensile strength, once these fibers do not have the role of improving the post-crack tensile parameters of concrete. Polypropylene micro-fibers were used only to reduce the risk of explosive spalling during heating procedure.

2.2. Composition and preparation of SFRC samples

The compositions employed in this study were developed taking as basis the concrete mix design focusing the requirements for the precast segments designed for the Subway Line 6, at São Paulo (Brazil). Table 1 shows the dosage of materials to produce 1 m^3 of each SFRC composition. In this work, the SFRC mix containing 20, 35 and 70 kg/m^3 that is equivalent to 0.26%, 0.45%, and 0.90% of steel fibers (by volume) were identified as SFRC-0.26, SFRC-0.45, and SFRC-0.90, respectively. Synthetic micro-fibers were added in a content of 0.09% of the total volume, or 0.8 kg/m^3, according to project specifications in order to avoid explosive spalling during heating process. Silica fume was used as supplementary cementitious material at a content of 5.5% of the cement

Table 3
Distribution of SRFC specimens according to mechanical tests.

Specimen type	Test	Property	Fiber content	Quantity
Cylindrical (Ø100x200 mm)	Compressive test	Compressive strength	0.26%	24*
			0.45%	24*
			0.90%	24*
		Elastic modulus	0.26%	24*
			0.45%	24*
			0.90%	24*
Cubic (100x100x100 mm)	DEWS test	Tensile properties	0.26%	60**
			0.45%	60**
			0.90%	60**

* 4 specimens for each target temperature: 25, 150, 300, 450, 600 and 750 °C.
** 10 specimens for each target temperature: 25, 150, 300, 450, 600 and 750 °C.

mass, and the w/c ratio was kept constant at 0.41. All the aggregates were employed in dried condition for the production of concrete and for that were oven-dried at 100 °C for 14 h before concrete production. The composite was prepared in a conventional concrete mixer (300 L capacity) at a room temperature of (24 ± 1) °C. The information regarding the granulation of the aggregates employed in this study are presented in Table 2. For further information and details regarding the properties of the materials employed and the mixing procedure, refer to Serafini et al. [17].

The consistency of the SFRC was determined by the Brazilian standard method ABNT NBR NM 67 which use the regular Abrams cone device [29] and the slump value was fixed at (40 ± 10) mm for the three concrete compositions, intended to be a C80 concrete. These measured results were obtained from the average calculated based in three determinations. The slump value was obtained for the three compositions by adjusting the superplasticizer content in the mixture (see Table 1).

The concrete produced was cast inside prismatic polypropylene molds with internal dimensions of 100 × 100 × 350 mm (width × height × length) and cylindrical steel molds with dimensions of Ø100 × 200 mm (diameter × height). The concrete consolidation was carried out through a vibratory table during 30 s with a frequency of 60 Hz. All specimens were cured in a saturated room for 72 h, and then stored at room temperature until the age of 150 days. Table 3 summarizes the distribution of the specimens produced in this study according to the mechanical tests and the different dosages. A total of 72 cylindrical specimens and 60 prismatic specimens were produced, distributed among the three contents of steel fibers used.

In sequence, all prismatic specimens were cut into cubic specimens with l = 100 mm to perform the DEWS test. The removal of cubic specimens from the prismatic ones and execution of the grooves/notches were conducted before the heating procedure. Fig. 2 illustrates the preparation of cubic specimens for the DEWS test [26]. The production of cubic specimens followed the procedure recommended by Borges et al. [30] and is summarized here for the convenience of the reader. Two triangular grooves with an inclination of 45° were cut along two opposite sides of the cubes in the face positioned 90° from the molding face and respecting the casting orientation, as shown in Fig. 2b. Then, two notches with a 5-mm depth and a 2-mm width were sawn, starting in the groove vertices towards the center of the cubes. The function of the notches is to induce the occurrence of the crack in the central portion of the cubic specimen.

2.3. Heating procedure

An industrial electric oven with maximum temperature of 1000 °C (INFORGEL GENGA model GCR.SP) was used to heat the cubic and cylindrical specimens. Fig. 3 shows the heating procedure adopted for cylindrical and cubic specimens. The variable heating rate capacity is a characteristic of electric ovens with a fix power capacity, since heating rate decreases as temperature increases [17]. The specimens were heated for target temperatures of 150, 300, 450, 600, and 750 °C and kept at each temperature during 10, 8, 6, 4, and 4 h, respectively. These target temperatures were chosen based on the analytical curves provided by the Eurocode [31] and CNR-DT 204 [32] guidelines, which show that the mechanical contribution for T ≥ 750 °C is considerably

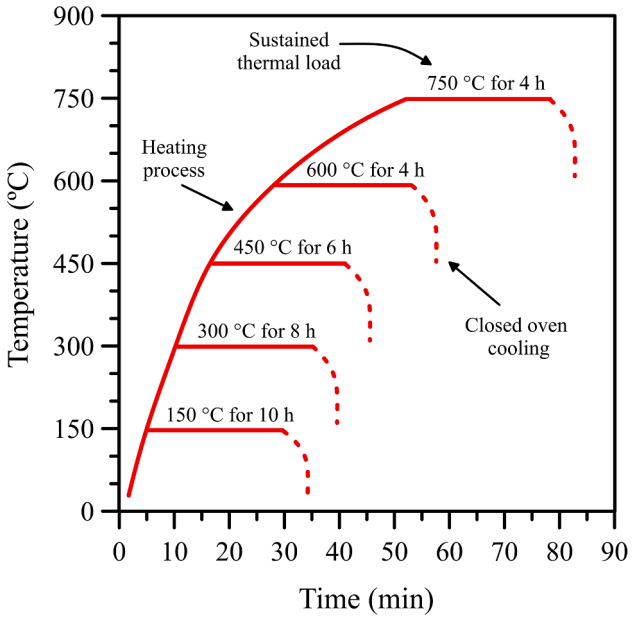

Fig. 3. Heating procedure adopted for cylindrical and cubic specimens.

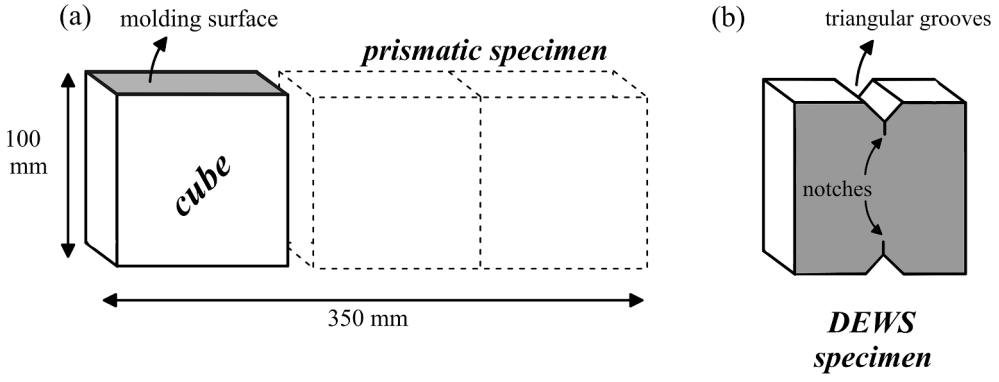

Fig. 2. Preparation of cubic specimens for the DEWS test [25].

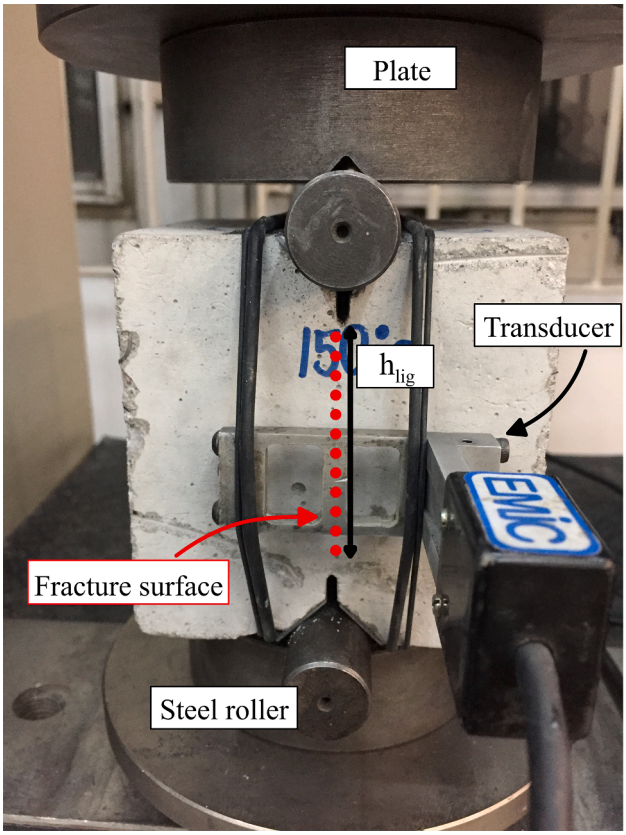

Fig. 4. The DEWS test setup adopted in this study.

low. In addition, the stabilization period was determined by numerical simulation to ensure the thermal stability of the specimens based on the work of Carpio et al. [33]. After the heat exposure was over, the chamber was kept closed and cooling until the room temperature was achieved for 24 h to avoid thermal shock. Then, the specimens were sealed in plastic bags in order to mitigate the chances of rehydration and were kept at this condition until the mechanical tests were to be conducted in according to the procedure adopted in previous study [34]. No explosive spalling was observed for all specimens.

2.4. Mechanical characterization

This section presents the mechanical tests adopted in this study. Results obtained in the mechanical characterization of SFRC were statistically evaluated through analysis of variance (ANOVA) and Tukey tests.

2.4.1. Determination of ultrasonic (US) pulse velocity

The determination of US pulse velocity was used to evaluate changes in terms of pore distribution and cracking caused by heat exposure. A Portable Ultrasonic Non-destructive Digital Indicating Tester (PUNDIT) equipment was employed for this evaluation and used 200 kHz transducers with a circular cross-section of 20 mm in diameter. The tests were conducted in one setting and the equipment was calibrated once before all tests were conducted, according to the specifications of the manufacturer. The US pulse velocity was determined in the same specimens before and after temperature exposure and used to determine the dynamic elastic modulus (E_d) of the concrete, calculated as:

$$E_d = \frac{\rho.V^2.(1+\mu)(1-2\mu)}{1-\mu} \quad (1)$$

where ρ is the density of the SFRC (in kg/m^3); V is the propagation pulse velocity (in km/s); μ is the Poisson's ratio. The density of the material was recalculated for each target temperature based on the mass and volume of the specimens. These values were updated to calculate the dynamic elastic modulus for each target temperature. The Poisson's ratio was assumed to be constant at 0.2 for all target temperatures, since it is a property that does not change significantly for small stress values [35].

2.4.2. Compressive strength and elastic modulus

The compressive strength (fc) and elastic modulus (Ec) of the SFRC were determined following the procedure presented by Brazilian standards [36,37]. The fc and Ec were determined employing four cylindrical specimens for each target temperature and steel fiber content (see Table 3). In addition, the coefficients of mechanical degradation for the compressive strength (K_c) and elastic modulus (K_{Ec}) were determined based on experimental results.

The tests were conducted in a Shimadzu Universal Testing Machine, model UH-2000kNXR, with a computer-controlled servo-hydraulic system, operating frequency of 60 Hz, and maximum load capacity of 2000 kN. The test was load-controlled at a rate of 0.5 MPa/s and the SFRC axial strain was determined by the average readings of two displacement transducers attached around the specimen. The elastic modulus was determined using the secant line between 0.5 MPa and 0.3 f_c and the respective deformation in the stress–strain curves. Only one loading cycle was performed in order to determine the elastic modulus, since the specimens were severely affected by temperature.

2.4.3. Double edge wedge splitting (DEWS) test

The DEWS test was employed to assess the tensile strength and post-crack tensile strength of oven-heated cubic specimens. On the test date, steel plates with thickness of 0.9 mm were glued to the surface of the specimens' grooves using body filler as glue, which has the function of reducing the friction interaction between the steel roller and the surface of the specimen during the test. In addition, graphite powder was applied to lubricate the contact between the roller and the steel plates as recommended by di Prisco et al. [26].

The DEWS test was conducted in an open-loop electromechanical universal test machine, EMIC DL 10000, with a load cell with maximum load capacity of 10 kN, and frame stiffness of 42 kN/mm. Two 50 mm length transducers were fixed with elastomeric straps in opposite faces of the cubic specimen, at half height and perpendicular to the fracture plane. The recorded crack opening displacement (COD) values are given by the arithmetic mean of the measurements obtained by the transducers. Tests were conducted using a COD opening displacement rate of 0.12 mm/min. This rate was adopted based on the study by Borges et al. [30], which concluded that it is possible to use a higher rate than that adopted by di Prisco et al. [26] without compromising the stress values obtained. Fig. 4 shows the DEWS test setup adopted in this study.

The load provided by the testing machine cannot be considered as the load in the specimen fracture surface due to the geometry of the specimens. Therefore, it is necessary to convert the load values obtained from the equipment (P) into the "splitting load" that effectively acts on the fracture surface (P_{ef}). Considering the equilibrium equations, di Prisco et al. [26] proposed the following equation to determine the actual "splitting load":

$$P_{ef} = P.\frac{(cos\theta - \mu sin\theta)}{(sin\theta + \mu cos\theta)} \quad (2)$$

where θ is the angle between the groove surface and the center line of the notch ($\theta = 45°$), and μ is the coefficient of friction between two steel surfaces lubricated with graphite ($\mu = 0.06$). The tensile stress (σ) was determined based on Equation (3), proposed by di Prisco et al. [26], where b is the depth of the specimen and h_{lig} is the height of the ligament (fracture surface).

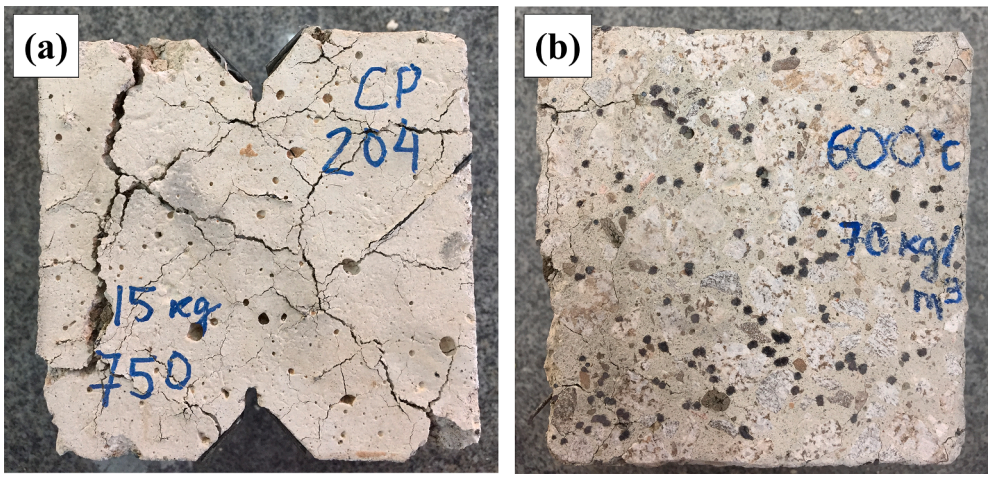

Fig. 5. (a) Cracked concrete after exposure to T = 750 °C, (b) oxidation of steel fibers in the cubic specimen.

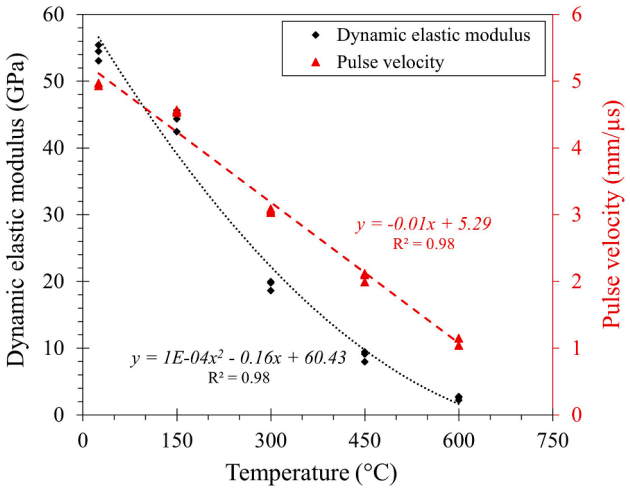

Fig. 6. Dynamic elastic modulus and US pulse velocity changes as a function of temperature.

$$\sigma = \frac{P_{ef}}{b.h_{lig}} \tag{3}$$

The post-crack tensile strength values associated to the service limit state (f_{Fts}) and to the ultimate limit state (f_{Ftu}) condition were adopted as the values associated to the crack opening displacement (COD) values of 0.25 mm and 1.25 mm, respectively. These values of COD were used based on the intrinsic geometrical differences in terms of test configuration and crack opening pattern between three-point flexural test and the DEWS test. Therefore, changes in the COD values for the DEWS test aim to obtain equivalence in terms of crack opening between the tests, according to the discussions proposed by Borges et al. [30] and Serafini et al. [25].

The coefficients of mechanical degradation for the tensile strength (K_{Ft}) and post-crack tensile strength associated to the ULS (K_{Ftu}) were determined based on experimental results obtained with the application of the DEWS test. These coefficients have a particular use for the assessment of fiber reinforced concrete structures by means of cross-sectional analysis [32].

2.5. Sample size and admissible error

As an additional investigation, the relationship between the sample size and the admissible error for the DEWS test was determined based on inferential statistics [38] and is presented in detail in Appendix A.

3. Results and discussion

3.1. Physical evaluation

Fig. 5 shows the crack pattern of SFRC after 750 °C and the oxidation of fibers. The SFRC was severely degraded by the exposure to elevated temperature, which may be attributed to the dehydration of hydrated products and the thermal stresses induced during the heat exposure [17]. Additionally, none of the specimens had cross-sectional losses due to the occurrence of explosive spalling, which may be attributed to the presence of micro-synthetic fibers in the mix design.

A dark layered formation was observed on the surface of the steel fibers after temperature exposure (see Fig. 5b). This dark layer resulted from an oxidation process that produces a three-layered scale structure made of wustite (FeO), hematite (Fe_2O_3), and magnetite (Fe_3O_4) [39]. This oxide layer formation results in an increase in mass and total diameter of the steel fibers (oxide + steel), however the steel portion of the cross-sectional area tends to reduce [40]. Moreover, the recrystallization of steel occurs at ~ 450 °C, which increases the grain sizes and reduce the grain boundary density of steel [41]. These physical and microstructural effects result in considerable tensile strength reductions of ~ 50% and ~ 90% for the respective temperatures of 400 and 650 °C [40].

3.2. US pulse velocity

Fig. 6 illustrates the dynamic elastic modulus and US pulse velocity changes as a function of temperature. The results show that the reductions in terms of pulse velocity are similar among samples with different fiber content, which indicates that there is no relation between fiber content and pulse velocity. In other words, it is possible to observe that the increase in fiber content did not increase the pulse velocity. This fact occurs because the relative volume of steel fibers used is very small (less than 1%) which is not significant to change the pulse velocity. This similarity in terms of pulse velocity values can be verified even for samples exposed to elevated temperatures. The pulse velocity reduced around 10%, 40%, 60%, and 80% after exposure to the respective temperatures of 150, 300, 450 e 600 °C, while the dynamic elastic modulus reduced around 20%, 65%, 85%, and 95%, respectively.

Moreover, the time required for pulse to propagate through the SFRC increases with temperature, which may be related to the increase in porosity and consequent delay of the ultrasonic pulse wave. In this sense, the US pulse velocity test may be employed as a tool to verify the damage in SFRC, since the test has a direct relationship with the density

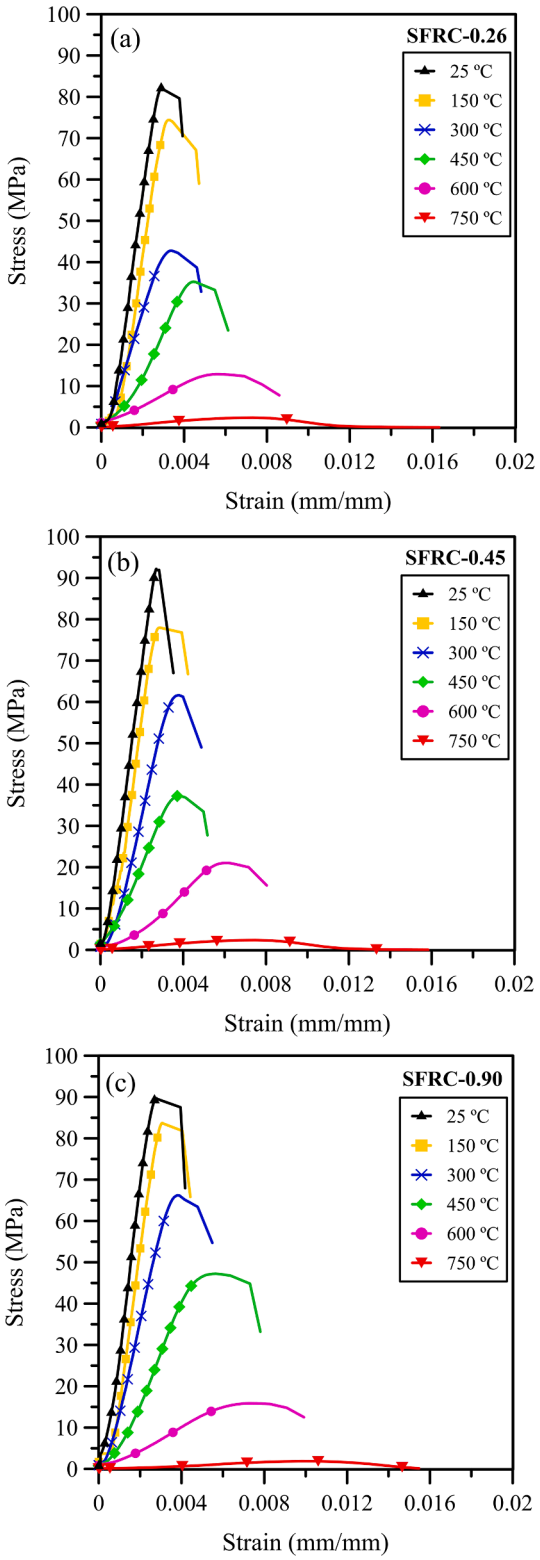

Fig. 7. Stress–strain curves as a function of temperature and fiber content of (a) 0.26%, (b) 0.45% and (c) 0.90%.

and elastic properties of the material. The determination of ultrasonic pulse velocity in specimens subjected to T ≥ 450 °C was difficulted due to the severe cracking that disturbs the US pulse transmission, which is also verified in literature [42]. The US pulse velocity for specimens exposed to temperatures of 750 °C was not determined due to compromised repeatability of the results.

Table 4
Average compressive strength and elastic modulus as a function of temperature.

Target temperature (°C)	SFRC identification	f_c (MPa)	Ec (GPa)
25	SFRC-0.26	84.8 (±2.1)	34.8 (±0.7)
	SFRC-0.45	91.8 (±2.1)	35.7 (±0.8)
	SFRC-0.90	90.8 (±1.1)	36.9 (±0.6)
150	SFRC-0.26	72.9 (±2.1)	25.7 (±0.5)
	SFRC-0.45	78.2 (±2.1)	27.1 (±0.3)
	SFRC-0.90	84.7 (±1.9)	28.9 (±0.4)
300	SFRC-0.26	44.2 (±1.3)	9.6 (±0.4)
	SFRC-0.45	62.5 (±1.7)	10.9 (±0.3)
	SFRC-0.90	66.9 (±1.7)	11.8 (±0.4)
450	SFRC-0.26	34.9 (±0.8)	3.6 (±0.2)
	SFRC-0.45	37.5 (±1.1)	4.3 (±0.2)
	SFRC-0.90	46.8 (±1.3)	4.4 (±0.2)
600	SFRC-0.26	13.1 (±0.3)	1.1 (±0.1)
	SFRC-0.45	19.8 (±0.7)	1.2 (±0.1)
	SFRC-0.90	16.9 (±0.4)	1.4 (±0.1)
750	SFRC-0.26	1.6 (±0.1)	0.1 (±0.1)
	SFRC-0.45	2.2 (±0.1)	0.3 (±0.1)
	SFRC-0.90	1.9 (±0.1)	0.4 (±0.1)

Additionally, the reduction in terms of mass values was similar between samples with different fiber content. After exposure to 750 °C, the mass values reduced around 10% when compared with room temperature results. The reduction in density with the increase in temperature is related mainly to the increase in porosity of the cement paste, the formation of an extensive crack network related with the thermal induced stresses, as well as the dehydration of hydrated products [43,44]. Moreover, the water located in the pore structure of concrete evaporates as the heating occurs, which also affects the density values.

3.3. Compressive strength and elastic modulus

Fig. 7 shows the compressive stress–strain curves as a function of temperature and fiber content. Table 4 shows the average compressive strength (f_c) values and elastic modulus (E_c) as a function of temperature. A significant reduction in compressive strength is verified for T ≥ 300 °C, which is related with the dehydration of hydrated products and the incompatibility in terms of thermal strain between the aggregates and the cement paste. This thermal incompatibility is also responsible for cracks in the interfacial transition zone between aggregates and the cement paste [25,43].

Fig. 8 shows the coefficients of reduction for f_c and E_c as a function of temperature. The coefficients of reduction for the compressive strength (K_c) and the elastic modulus (K_{Ec}) obtained in this study are lower than those prescribed by the Eurocode [31]. This means that the reduction of f_c and E_c obtained in this study was higher than those prescribed in European guidelines, which may suggest that the curves provided in Eurocode may be out of the safe condition for this particular case. The results obtained in this study also differ from some studies found in literature for similar class of concrete with similar fiber content [45–52]. However, the results presented in this paper agree well with some recently published studies that employed longer heat regimes to ensure the thermal stability of the SFRC [17,25]. In this sense, the differences when compared to Eurocode and some studies in literature may be a result from the heat regime adopted, which ensured temperature uniformity within the entire volume of the specimens, as well as the increase in porosity caused by the ignition of the micro synthetic fibers.

The use of higher fiber content mitigated the reductions in f_c for T ≤ 450 °C. In this sense, the SFRC-0.90 showed a reduction rate of ~ 0.10 MPa/°C, while the samples SFRC-0.26 and SFRC-0.45 have shown reductions ranging between 0.15 and 0.20 MPa/°C in the range of 25 °C ≤ T ≤ 450 °C. Therefore, the reductions in terms of f_c for SFRC-0.90 were about 10% lower than those obtained for SFRC-0.26 and SFRC-0.45. This favorable effect of fibers was also verified in the work of Chan et al. [45] and Felicetti et al. [46].

The slightly increased compressive capacity for SFRC-0.90 in

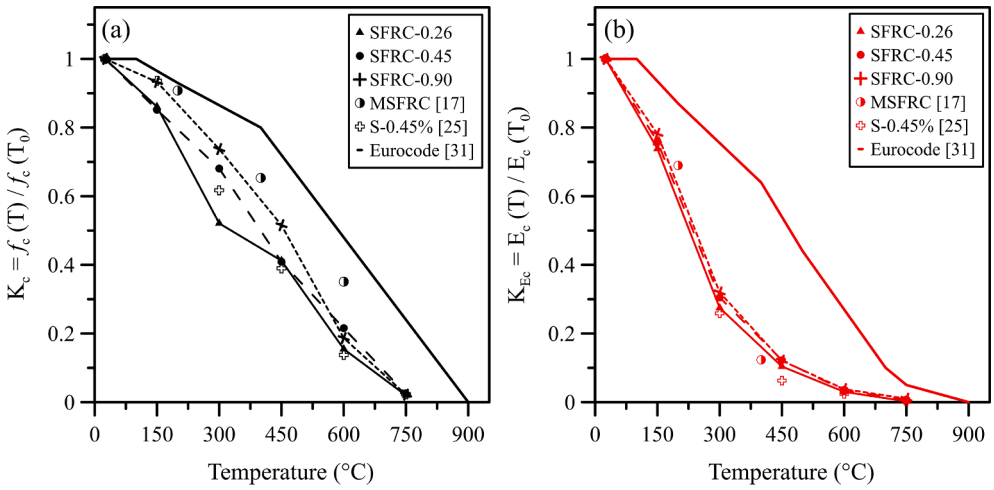

Fig. 8. Coefficients of reduction for the (a) compressive strength and (b) elastic modulus as a function of temperature.

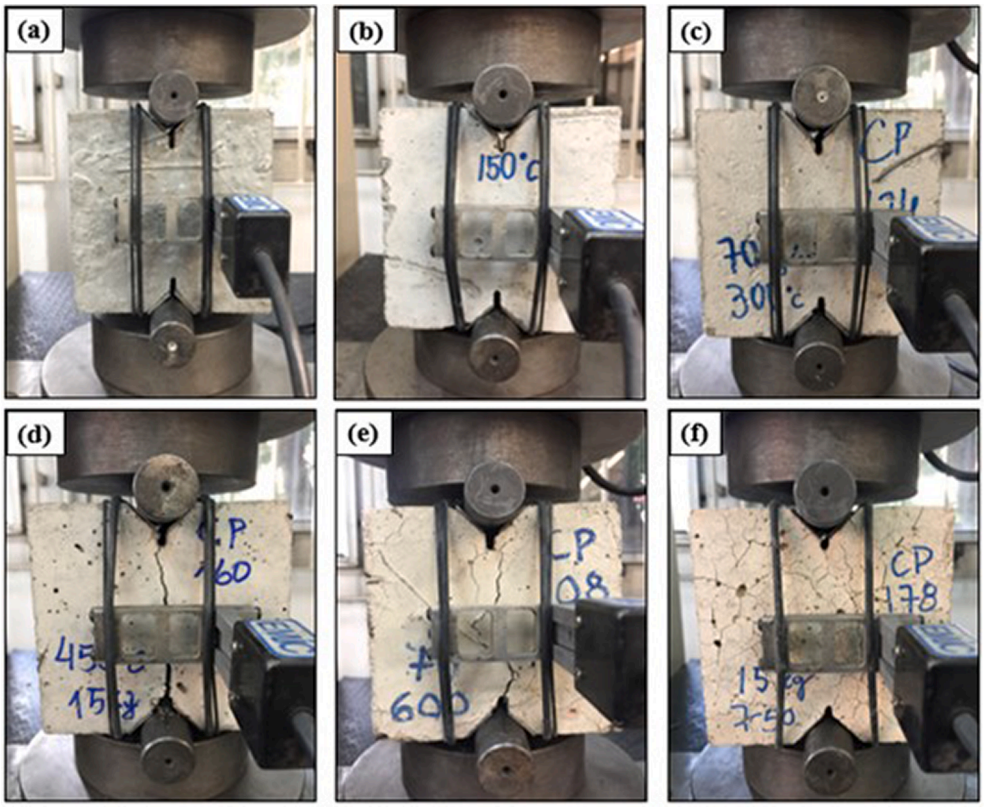

Fig. 9. The DEWS test and the integrity condition of the SFRC samples exposed to (a) room temperature, (b) 150 °C, (c) 300 °C, (d) 450 °C, (e) 600 °C, and (f) 750 °C.

elevated temperatures up to 450 °C may occur due to the increase in the amount of energy required for the unstable rupture of concrete, which is related to the fundamental bridging mechanism of steel fibers [53]. Notice that the peak load was obtained for greater displacement values for SFRC-0.90 than for the SFRC-0.26 and SFRC-0.45. In this sense, the increase in fiber content increases the deformation capacity of the material, since the maximum stress level would be associated with a greater strain value (see Fig. 7). Therefore, the increase in fiber content may mitigate the reductions in f_c after temperature exposure fundamentally by improving the bridging mechanism through the cracks. This tendency may be justified by the negligible effect of temperature on the bond-slip behavior of steel fibers up to $T \leq 450$ °C [34]. For $T = 600$ °C all the samples retained ~ 20% of their initial f_c, independently of the fiber content employed, while at $T = 750$ °C the f_c may be considered practically zero.

The reductions in the values of E_c were more severe than those obtained for f_c, independently of the fiber content. After exposure to $T = 450$ °C, the SFRC retained only ~ 15% of the result obtained at room temperature. This suggests that the elastic properties are not influenced by fiber content, which was also pointed out by Yermak et al. [48]. In this sense, the major factors influencing the reduction in the elastic properties of the SFRC may be related to the reduction in the volume of solids in the cement paste, the increase in the porosity of aggregates [43], and the dehydration of hydrated products [54,55]. Some additional factors can be mentioned, such as the thermal related cracking and the deterioration of the micro-synthetic fibers [17,25].

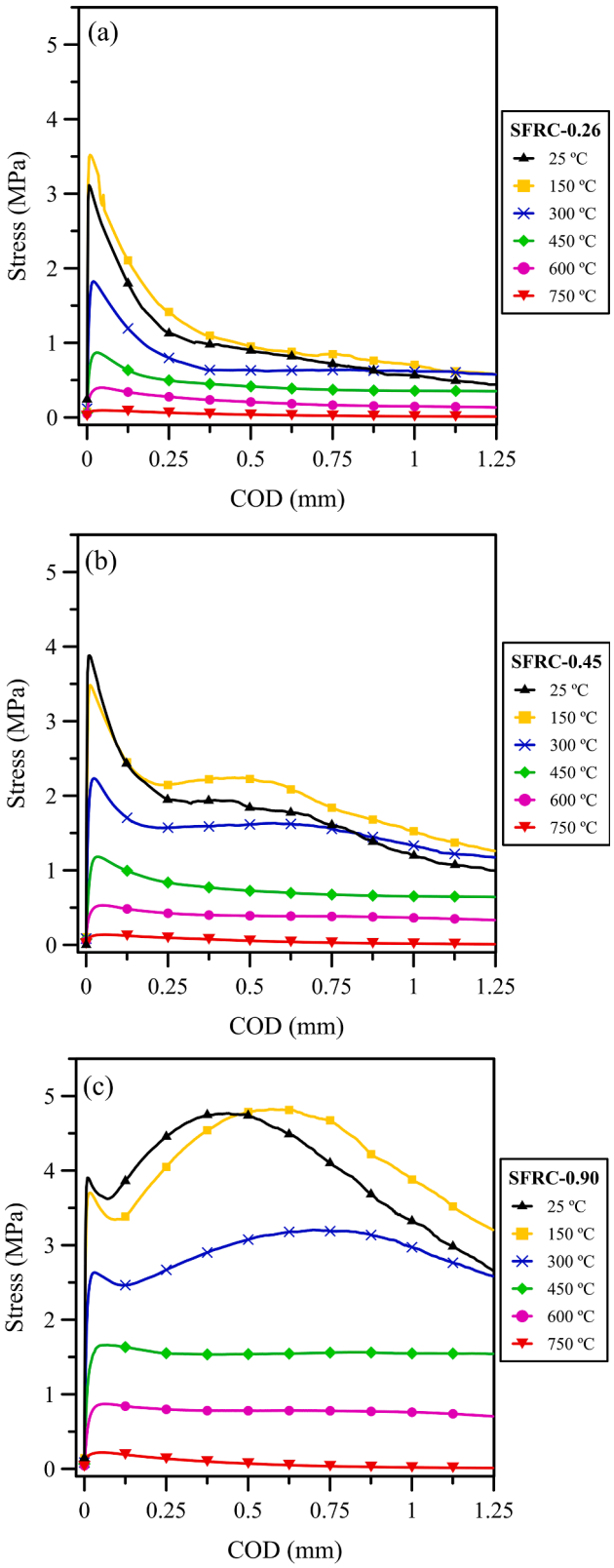

Fig. 10. Average stress-COD curves for the (a) SFRC-0.26, (b) SFRC-0.45, and (c) SFRC-0.90 samples.

3.4. Tensile properties of the SFRC

Fig. 9 illustrates the DEWS test and the integrity condition of the SFRC samples. No grinding or damage was verified in the contact between the roller and the specimen, while the crack opening was similar in both faces of the sample. In all cases the failure mode consisted of a single vertical crack between the notches (mode I fracture).

Table 5
Average results in terms of tensile and post-crack tensile strength for SFRC.

Target temperature (°C)	SFRC identification	f_{Ft} (MPa)	f_{Fts} (MPa)	f_{Ftu} (MPa)
25	SFRC-0.26	3.1 (±0.7)	1.2 (±0.9)	0.4 (±0.4)
	SFRC-0.45	3.8 (±0.7)	2.0 (±0.3)	1.0 (±0.2)
	SFRC-0.90	3.9 (±0.7)	4.4 (±0.9)	2.6 (±0.7)
150	SFRC-0.26	3.5 (±0.4)	1.5 (±0.8)	0.6 (±0.3)
	SFRC-0.45	3.5 (±0.8)	2.1 (±0.8)	1.3 (±0.3)
	SFRC-0.90	3.7 (±0.7)	4.1 (±0.7)	3.2 (±1.2)
300	SFRC-0.26	1.8 (±0.3)	0.8 (±0.2)	0.6 (±0.3)
	SFRC-0.45	2.3 (±0.4)	1.6 (±0.5)	1.2 (±0.5)
	SFRC-0.90	2.6 (±0.3)	2.7 (±0.5)	2.6 (±0.9)
450	SFRC-0.26	0.9 (±0.3)	0.5 (±0.2)	0.3 (±0.2)
	SFRC-0.45	1.2 (±0.2)	0.8 (±0.2)	0.6 (±0.2)
	SFRC-0.90	1.7 (±0.3)	1.5 (±0.3)	1.5 (±0.4)
600	SFRC-0.26	0.4 (±0.1)	0.3 (±0.1)	0.1 (±0.1)
	SFRC-0.45	0.5 (±0.2)	0.4 (±0.1)	0.3 (±0.1)
	SFRC-0.90	0.9 (±0.2)	0.8 (±0.2)	0.7 (±0.1)
750	SFRC-0.26	0.1 (±0.1)	0.1 (±0.1)	0.1 (±0.1)
	SFRC-0.45	0.1 (±0.1)	0.1 (±0.1)	0.1 (±0.1)
	SFRC-0.90	0.2 (±0.1)	0.2 (±0.1)	0.1 (±0.1)

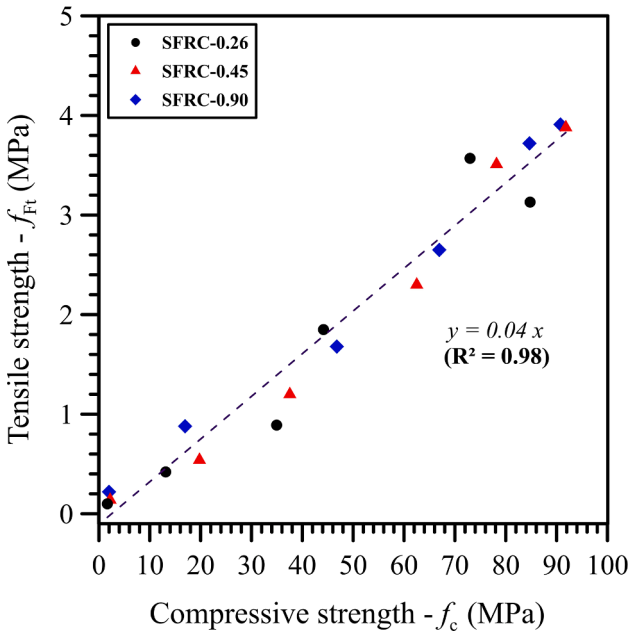

Fig. 11. Correlation between f_{Ft} and f_c for all the temperatures evaluated in this study.

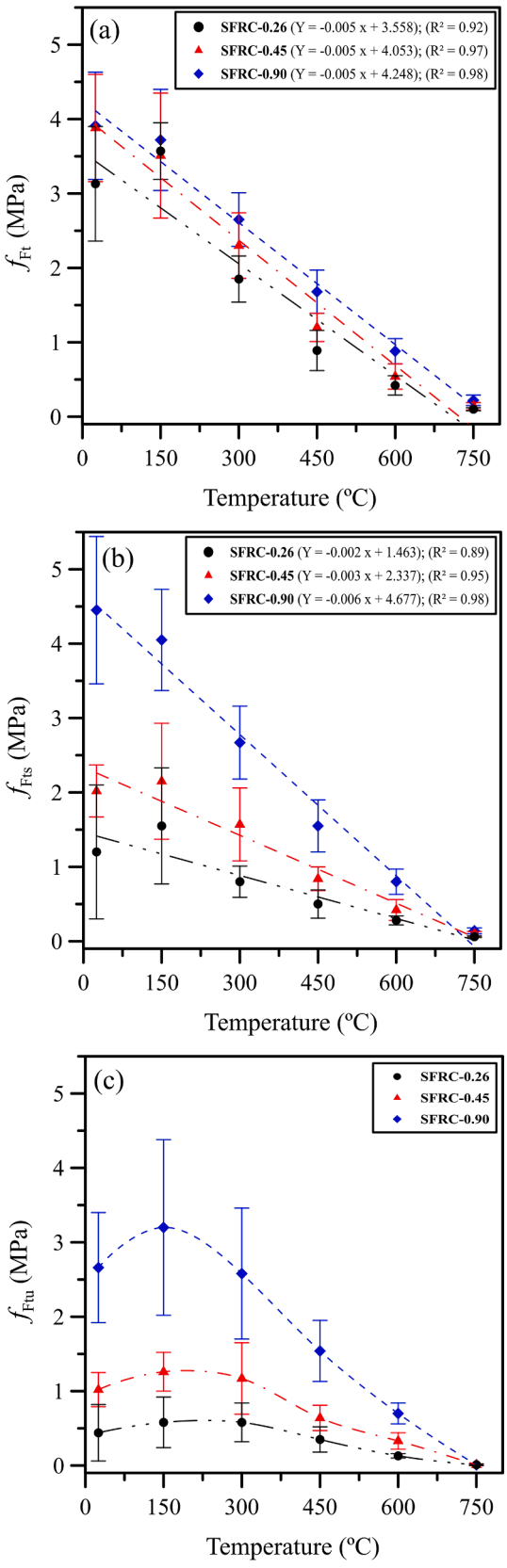

Fig. 12. Correlation between stress values and target temperatures: (a) f_{Ft}, (b) f_{Fts}, and (c) f_{Ftu}.

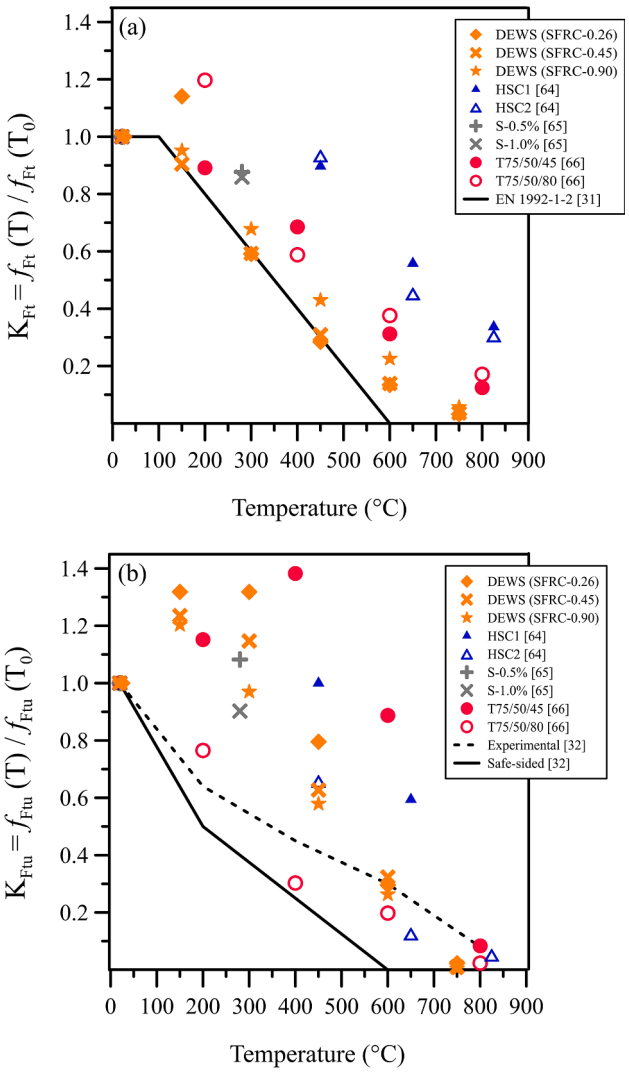

Fig. 13. Coefficients of mechanical degradation for (a) f_{Ft} and (b) f_{Ftu} compared to European standards.

Moreover, the crack opening in both sides of the specimens was similar, which is a first indicative that the methodology may be applied to SFRC after temperature exposure.

Fig. 10 shows the average stress-COD curves for the SFRC-0.26, SFRC-0.45, and SFRC-0.90 samples. The average values of f_{Ft}, f_{Fts} and f_{Ftu} are presented in Table 5, with the standard deviation values in the parenthesis. A significant reduction in f_{Ft} is verified for T $\geq$ 300 °C, which is related to the dehydration of hydrated products and the changes in the pore distribution of the cement paste and aggregates [17,25,44]. The deterioration process is further aggravated by the micro-cracking process that affects the cementitious matrix and aggregates due to the expansive transition from α-quartz (trigonal) to β-quartz (hexagonal) for T $\geq$ 573 °C [56].

The f_{Ft} values were not significantly affected for T $\leq$ 150 °C, independently of the fiber content. The SFRC-0.90 maintained ~ 45% and ~ 25% of their initial f_{Ft} value after exposure to the respective temperatures of 450 and 600 °C, while the SFRC-0.26 and SFRC-0.45 maintained only ~ 30% and ~ 15%, respectively. This indicates that the steel fibers may have acted in controlling the thermal cracking process, which mitigates the reductions in f_{Ft} related to room temperature. However, the results obtained for T = 750 °C corresponded to ~ 5% of the f_{Ft} obtained at room temperature for all samples evaluated in this study, which may be attributed to the extensive degradation of the cementitious matrix and the fiber-paste interfacial transition zone [34].

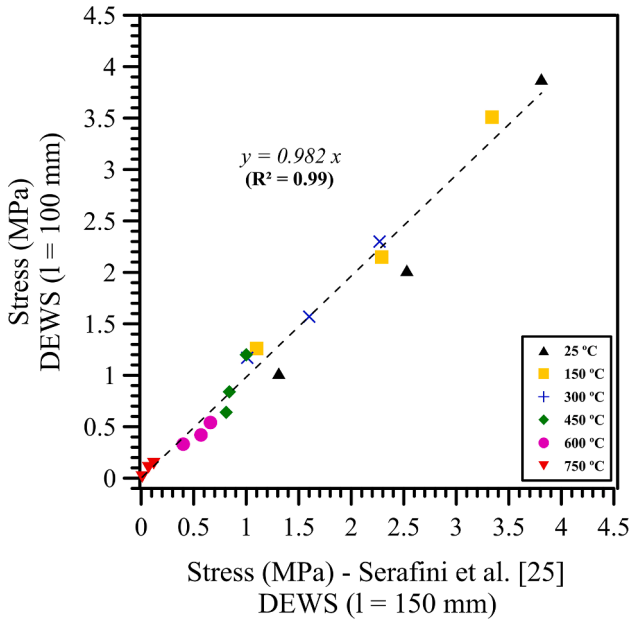

Fig. 14. Relationship in terms of f_{Ft}, f_{Fts} e f_{Ftu} between the results obtained in this study and the results obtained by Serafini et al. [25].

Fig. 11 shows the correlation between f_{Ft} and f_c for all the temperatures evaluated in this study. In average, the tensile strength represented ~ 4% of the compressive strength value, independently of the fiber content ($R^2 = 0.98$), while results found in classical literature for bending tests points out that the relation between f_{Ft} / f_c is ~ 10% [48,57–59]. This occurs because the tensile response of the material varies according to the test method employed. For example, the bending test induces a compressive region in the cross-section, which is known to increase the flexural tensile strength values [60]. Thus, the f_{Ft} / f_c obtained in this study seem to be reasonable considering that the DEWS test induces a mode I fracture with negligible compressive stresses in the fracture surface.

Moreover, the post-peak instability that is inherent to the evaluation of SFRC in open-loop control systems reached maximum COD values of over 0.3 mm during the DEWS test, especially for T ≤ 150 °C and for SFRC-0.26 (see Table 5). Even with this limitation, the post-peak instability reduced for samples with higher fiber content (*i.e.* SFRC-0.90) and after exposure to temperature, since the reduction in the gap between f_{Ft} and f_{Fts} occurred.

The f_{Fts} and f_{Ftu} values were not significantly affected for T ≤ 300 °C, which may be related with the minimal effect of temperature on the bond-slip behavior of hooked-end steel fibers at this temperature range [34,61–63]. A recent study published by Serafini et al. [34] showed that the fiber–matrix bond strength may increase up to ~ 40% for T ≤ 450 °C, which may be related with the densification of the ITZ and formation of C-S-H in this region due to an autoclave condition. In this sense, the reduction in f_{Ft} and the increase in f_{Fts} and f_{Ftu} for T ≤ 450 °C obtained in this study may be justified by the minimal or even beneficial effect of temperature on the bond-slip behavior of hooked-end steel fibers.

All the samples evaluated retained, respectively, ~20% and ~ 30% of f_{Fts} and f_{Ftu} after exposure to 600 °C. After exposure to 750 °C, only ~ 5% of f_{Fts} and f_{Ftu} was retained, independently of the fiber content. The reductions in post-crack tensile properties of SFRC are related to the loss of anchorage of the hooks, reduction of the mechanical properties of the steel fiber, and deterioration of the cementitious matrix and the fiber–matrix ITZ [34,61–63].

The increase in fiber content resulted in an increase in the post-crack tensile strength of the SFRC, independently of the target temperature evaluated. However, the reductions in terms of f_{Ftu} were similar between all the samples evaluated when compared to room temperature results. Additionally, the values of f_{Ft} and f_{Fts} tend to reduce linearly with temperature increase, while the f_{Ftu} values show a non-linear trend (see Fig. 12). Therefore, it is possible to observe that the reduction in terms of f_{Ftu} is negligible for T ≤ 300 °C and presents a linear reduction trend for greater temperature values. Also, the correlation between f_{Ftu} and temperature becomes more evident with the increase in fiber content.

Fig. 13 shows the coefficients of mechanical degradation for f_{Ft} and f_{Ftu} compared to European standards [31,32] and others results in the literature [64–66]. These coefficients may be used as reduction factors for the assessment of SFRC structures affected by fire. It is possible to observe that the f_{Ft} and f_{Ftu} values obtained in this study are in line with the analytical curves presented in European standards. The coefficient of mechanical degradation for f_{Ftu} (K_{Ftu}) is considerably greater than those prescribed by the CNR DT 204 [32]. This is also observed for the coefficients of mechanical degradation of literature results employing bending tests and a CMOD = 2.5 mm [64–66].

A considerable amount of studies may be found in literature employing bending tests, as well as different classes of concrete, steel fiber type, and heat regimes [48,51,67]. Since these factors may limit the comparison with the literature, the results obtained in this study are compared with the study of Serafini et al. [25]. However, Serafini et al. [25] conducted the DEWS test using cubic specimens with l = 150 mm, contrary to the current study that employed cubes with l = 100 mm. In this sense, a direct comparison was conducted in terms of stresses.

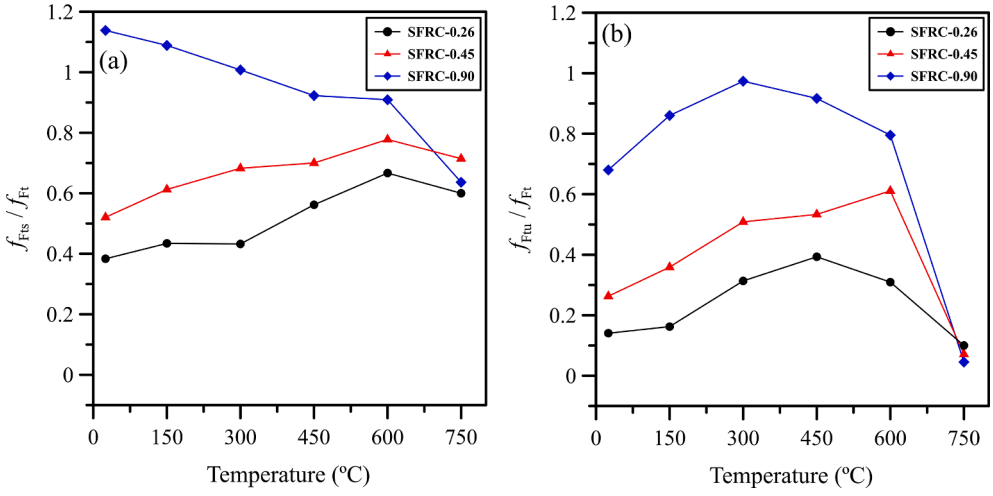

Fig. 15. Effect of temperature in the ductility parameters at the (a) SLS and (b) ULS.

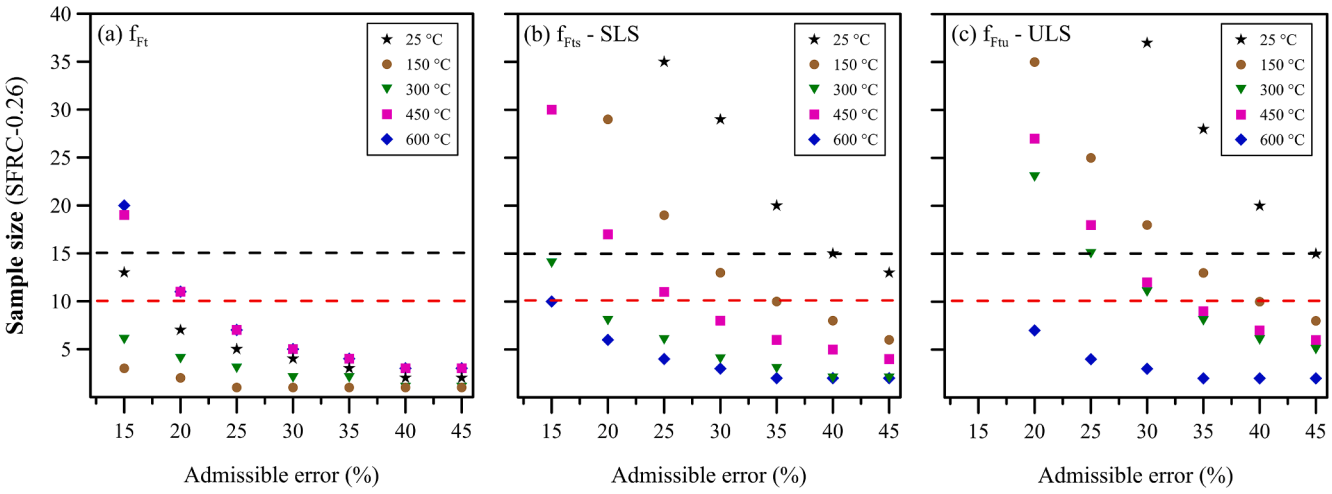

Fig. A1. SFRC-0.26: sample size required as a function of admissible error for (a) f_{Ft}, (b) f_{Fts}, and (c) f_{Ftu}.

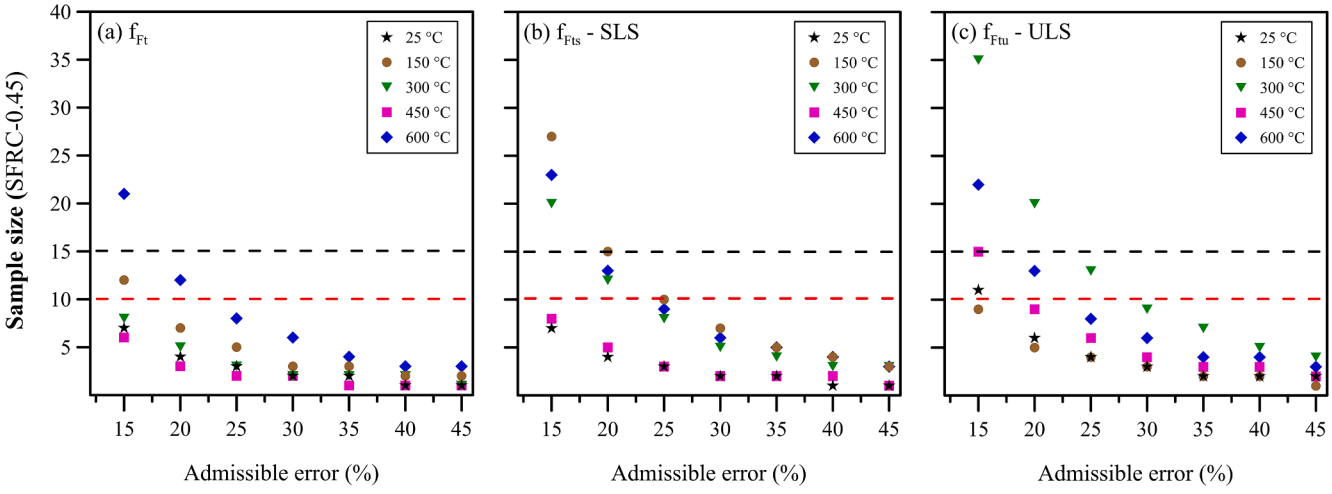

Fig. A2. SFRC-0.45: sample size required as a function of admissible error for (a) f_{Ft}, (b) f_{Fts}, and (c) f_{Ftu}.

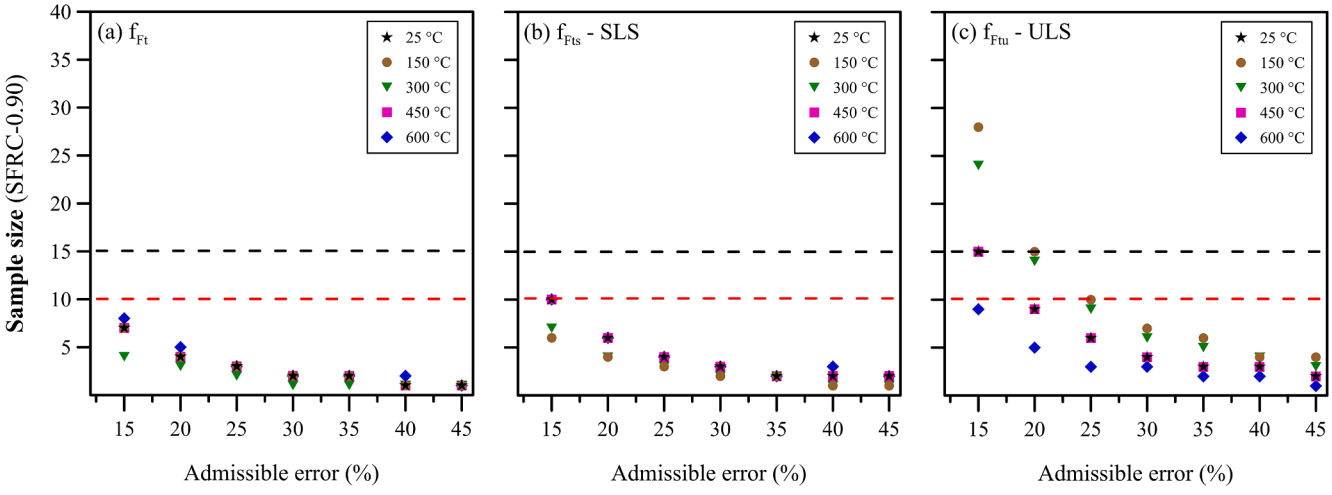

Fig. A3. SFRC-0.90: sample size required as a function of admissible error for (a) f_{Ft}, (b) f_{Fts}, and (c) f_{Ftu}.

Fig. 14 shows the relationship in terms of f_{Ft}, f_{Fts} and f_{Ftu} between the results obtained in this study and the results obtained by Serafini et al. [25]. Despite the significant differences in terms of specimens' size, the results seem to be comparable in terms of f_{Ft}, f_{Fts} e f_{Ftu} values. Moreover, a well-defined correlation ($R^2 = 0.99$) between the results obtained with cubes of l = 150 mm and l = 100 mm is verified. In this sense, the conversion factor between the specimens with different sizes is close to 1.0. These results suggest that the DEWS test may be employed in

reduced specimen size without compromising the reliability of the tensile results obtained.

In this context, the results point out that the use of specimens with l = 100 mm may be a feasible alternative to determine the tensile properties of the SFRC exposed to elevated temperatures. More than that, the analysis conducted in this study shows that the DEWS test yields representative results of the tensile properties of the composite, even after exposure to elevated temperatures. This is a valuable result considering that other test methods have shown limited applications when applied to the post-heat assessment of SFRC, such as the DPT test [24].

The values of f_{Ft} and the post-crack parameters were negatively affected by temperature following a linear trend with different rates of reduction. This resulted in a significant increase in terms of ductility up to 450 °C with the material behaving more closely as a perfect elasto-plastic material (see Fig. 15). Even with this post-fire ductility gain, it is important to highlight that the tensile properties of the composite are negatively affected by temperature, which affects the safety conditions of a structure.

4. Conclusions

The present study evaluated the effect of steel fiber content on the mechanical behavior of SFRC exposed to elevated temperatures. The main conclusions of this study showed that the use of steel fibers reduced the degradation rate of the SFRC in terms of the basic properties such as compressive strength and elastic modulus, which demonstrates that the European guides are in favor of safety in this aspect. The residual strength reduction rates, which are fundamental parameters for the structural application of the SFRC, are in an opposite direction since the values obtained were higher than those considered in the European guides. Complementarily, the following specific conclusions can be highlighted:

- The use of higher fiber content mitigated the reductions in f_c for T ≤ 450 °C. The SFRC-0.90 showed a reduction rate of ~ 0.10 MPa/°C, while the SFRC-0.26 and SFRC-0.45 have shown reductions ranging between 0.15 and 0.20 MPa/°C in the range of 25 °C ≤ T ≤ 450 °C. However, for T = 600 °C all the samples retained ~ 20% of their initial f_c, independently of the fiber content employed, while at T = 750 °C the f_c may be considered practically zero.
- As the temperature increased, the reductions in the values of E_c were similar among samples with different contents of steel fiber. After exposure to T = 450 °C, the SFRC retained only ~ 15% of the E_c obtained at room temperature. The rate of degradation presented for f_c and E_c was higher than the values provided by the Eurocode. This means that the reduction of f_c and E_c obtained in this study was higher than those prescribed in European guidelines, which should be used with caution when using materials in conditions similar to this experimental study.
- The increase in fiber content resulted in a reduction in the rate of f_{Ft} degradation. SFRC-0.90 samples maintained ~ 45% and ~ 25% of their initial f_{Ft} value after exposure to the respective temperatures of 450 and 600 °C, while SFRC-0.26 and SFRC-0.45 samples maintained only ~ 30% and ~ 15% for the same respective temperatures. However, the results obtained for T = 750 °C corresponded to ~ 5% of the f_{Ft} obtained at room temperature for all samples, regardless of the fiber content used.
- The reductions in the post-crack strength values did not occur with the same intensity as the reductions in f_{Ft}. The reductions in terms of f_{Ftu} were similar between all the samples evaluated when compared to room temperature results. All the samples evaluated retained ~ 30% of f_{Ftu} after exposure to 600 °C. After exposure to 750 °C, only ~ 5% of f_{Ftu} was retained, independently of the fiber content.
- The coefficients of mechanical degradation for f_{Ft} and f_{Ftu} were comparable to the patterns presented by European standards. The values obtained in this study for f_{Ft} and f_{Ftu} were higher than the values predicted by European guidelines, which suggests that the analytical curves prescribed by the guidelines are in favor of safety. There are limited guidelines regarding the effect of temperature on the post-crack tensile properties [32]. In this sense, this work contributes to the definition of design-oriented parameters for f_{Ftu} after temperature exposure.
- The DEWS test proved to be effective in evaluating the post-crack behavior of SFRC exposed to high temperatures, constituting a technically viable methodology under these conditions. No grinding or damage was verified in the contact between the roller and the specimen, while the crack opening pattern was similar at both faces of the specimens. Therefore, the DEWS test yields representative results of the tensile properties of the composite, even after exposure to elevated temperatures and for the fiber content range evaluated in this study.

The results obtained in this study can be used for the elaboration of constitutive equations and will serve as input data in numerical models for predicting the behavior of structural elements performed with SFRC, analyzing their performance level according to the steel fiber content adopted. Therefore, these results are a reference for the definition of safety parameters for the SFRC elements.

CRediT authorship contribution statement

Data curation, Formal analysis, Investigation, Methodology, Supervision, Validation, Writing – review & editing.

Declaration of Competing Interest

The authors declare that they have no known competing financial interests or personal relationships that could have appeared to influence the work reported in this paper.

Acknowledgments

The first and second authors would like to thank the Institute for Technological Research (IPT) and its foundation (FIPT) for their financial and institutional support though the New Talents Program N.01/2017 and N.01/2018, respectively. This work was partially supported by the Conselho Nacional de Desenvolvimento Científico e Tecnológico (CNPq) [Grant # 305055/2019-4 (Antonio Domingues de Figueiredo)]. The authors would also like to thank Dra. Renata Monte for the technical contributions that improved the quality of this work.

Appendix A

Sample size and admissible error

The relationship between the sample size and the admissible error for the DEWS test was determined based on concepts of inferential statistics according to:

$$n = \frac{s^2 . z_\gamma{}^2}{\varepsilon^2} \quad \text{(A1)}$$

where n is the number of specimens required (sample size); s is the standard deviation obtained by the pilot sample (in MPa); z_γ is the t-Student distribution value; and ε is the admissible error for the test. The average values and the standard deviation were determined based on the experimental results, while $z_\gamma = 2{,}132$ was adopted considering a confidence interval of 95% and (n-1) degrees of freedom.

Results obtained

Figs. A1, A2, and A3 present the sample size as a function of admissible error for the tensile properties of SFRC-0.26, SFRC-0.45, and SFRC-0.90, respectively. The results show that the number of required samples increases with the reduction of the admissible error for the DEWS test. For the f_{Ft} of the SFRC-0.26, using 10 cubes results in a maximum admissible error of ~ 25%, however the variability in the post-crack tensile properties (*i.e.* f_{Fts} and f_{Ftu}) increases the sample size to over 35 specimens for the same admissible error. Contrarily, the SFRC-0.45 requires 15 cubic specimens to ensure a maximum admissible error of ~ 25% for all the tensile properties of the composite, which occurred because the increase in fiber content reduced the variability in the f_{Fts} and f_{Ftu} values. Lastly, the SFRC-0.90 requires 10 cubic specimens to ensure an admissible error of 25% for all tensile properties of SFRC.

In this sense, it is possible to observe that the increase in fiber content reduces the variability of f_{Fts} and f_{Ftu}, which results in the reduction of the sample size required to ensure the same admissible error. Moreover, the increase in temperature seem to negatively affect the dispersion of results, with an exception to the SFRC-0.26. Therefore, the data provided in this section may serve as a reference for the definition of sample sizes for future studies that are going to employ the DEWS test to characterize a SFRC.

References

[1] fib, fib Model Code for Concrete Structures 2010, Wiley-VCH Verlag GmbH & Co. KGaA, Weinheim, Germany, 2013. https://doi.org/10.1002/9783433604090.

[2] X. Destrée, J. Mandl, Steel fibre only reinforced concrete in free suspended elevated slabs, in: Tailor Made Concr. Struct., CRC Press, 2008: pp. 111–111. https://doi.org/10.1201/9781439828410.ch74.

[3] J.A.O. Barros, H. Salehian, N.M.M. A Pires, D.M.F. Gonçalves, Design and testing elevated steel fibre reinforced self-compacting concrete slabs, 8th RILEM Int. Symp. Fiber Reinf. Concr. Challenges Oppor. (BEFIB 2012). (2012) 1–12.

[4] F. Dehn, A. Herrmann, Concreto reforçado com fibra de aço (SFRC) em situação de incêndio – requisitos normativos, pré-normativos e códigos-modelo, Concreto Construções 87 (2017).

[5] R.R. Agra, R. Serafini, A.D. de Figueiredo, Fiber Reinforced Concrete After Elevated Temperatures: Techniques of Characterization, in: Fibre Reinf. Concr. Improv. Innov., Springer Nature, 2021: pp. 233–244. https://doi.org/10.1007/978-3-030-58482-5_21.

[6] A.-A. Alyaa A., A. Mazin B., H. Hussein M., T. Bassam A., Investigating the behaviour of hybrid fibre-reinforced reactive powder concrete beams after exposure to elevated temperatures, J. Mater. Res. Technol. 9 (2020) 1966–1977. https://doi.org/10.1016/j.jmrt.2019.12.029.

[7] M. Amin, B.A. Tayeh, I. saad Agwa, Investigating the mechanical and microstructure properties of fibre-reinforced lightweight concrete under elevated temperatures, Case Stud. Constr. Mater. 13 (2020) e00459. https://doi.org/10.1016/j.cscm.2020.e00459.

[8] Mahdi Nematzadeh, Morteza Tayebi, Hojjat Samadvand, Prediction of ultrasonic pulse velocity in steel fiber-reinforced concrete containing nylon granule and natural zeolite after exposure to elevated temperatures, Constr. Build. Mater. 273 (2021) 121958, https://doi.org/10.1016/j.conbuildmat.2020.121958.

[9] Maziar Fakoor, Mahdi Nematzadeh, A new post-peak behavior assessment approach for effect of steel fibers on bond stress-slip relationship of concrete and steel bar after exposure to high temperatures, Constr. Build. Mater. 278 (2021) 122340, https://doi.org/10.1016/j.conbuildmat.2021.122340.

[10] M. Nematzadeh, A. Karimi, A. Gholampour, Pre- and post-heating behavior of concrete-filled steel tube stub columns containing steel fiber and tire rubber, Structures 27 (2020) 2346–2364, https://doi.org/10.1016/j.istruc.2020.07.034.

[11] Mazin Abdul-Rahman, Alyaa A. Al-Attar, Hussein M. Hamada, Bassam Tayeh, Microstructure and structural analysis of polypropylene fibre reinforced reactive powder concrete beams exposed to elevated temperature, J. Build. Eng. 29 (2020) 101167, https://doi.org/10.1016/j.jobe.2019.101167.

[12] James H. Haido, Bassam A. Tayeh, Samadar S. Majeed, Mehmet Karpuzcu, Effect of high temperature on the mechanical properties of basalt fibre self-compacting concrete as an overlay material, Constr. Build. Mater. 268 (2021) 121725, https://doi.org/10.1016/j.conbuildmat.2020.121725.

[13] Nur Khaida Baharuddin, Fadzli Mohamed Nazri, Badorul Hisham Abu Bakar, Salmia Beddu, Bassam A. Tayeh, Potential use of ultra high-performance fibre-reinforced concrete as a repair material for fire-damaged concrete in terms of bond strength, Int. J. Integr. Eng. 12 (9) (2020), https://doi.org/10.30880/ijie10.30880/ijie.2020.12.0910.30880/ijie.2020.12.09.011.

[14] Hamed Jafarzadeh, Mahdi Nematzadeh, Evaluation of post-heating flexural behavior of steel fiber-reinforced high-strength concrete beams reinforced with FRP bars: experimental and analytical results, Eng. Struct. 225 (2020) 111292, https://doi.org/10.1016/j.engstruct.2020.111292.

[15] Mahdi Nematzadeh, Armin Memarzadeh, Amirhossein Karimi, Post-fire elastic modulus of rubberized fiber-reinforced concrete-filled steel tubular stub columns: experimental and theoretical study, J. Constr. Steel Res. 175 (2020) 106310, https://doi.org/10.1016/j.jcsr.2020.106310.

[16] A. Karimi, M. Nematzadeh, S. Mohammad-Ebrahimzadeh-Sepasgozar, Analytical post-heating behavior of concrete-filled steel tubular columns containing tire rubber, Comput. Concr. 26 (2020) 467–482.

[17] R. Serafini, S.R.A. Dantas, R.P. Salvador, R.R. Agra, D.A.S. Rambo, A.F. Berto, A. D. de Figueiredo, Influence of fire on temperature gradient and physical-mechanical properties of macro-synthetic fiber reinforced concrete for tunnel linings, Constr. Build. Mater. 214 (2019) 254–268, https://doi.org/10.1016/j.conbuildmat.2019.04.133.

[18] R. Qiao, Z. Shao, F. Liu, W. Wei, Damage evolution and safety assessment of tunnel lining subjected to long-duration fire, Tunn. Undergr. Sp. Technol. 83 (2019) 354–363, https://doi.org/10.1016/j.tust.2018.09.036.

[19] F. Di Carlo, A. Meda, Z. Rinaldi, Evaluation of the bearing capacity of fiber reinforced concrete sections under fire exposure, Mater. Struct. 51 (2018) 154, https://doi.org/10.1617/s11527-018-1280-2.

[20] S. Ahmad, M. Rasul, S.K. Adekunle, S.U. Al-Dulaijan, M. Maslehuddin, S.I. Ali, Mechanical properties of steel fiber-reinforced UHPC mixtures exposed to elevated temperature: effects of exposure duration and fiber content, Compos. Part B Eng. 168 (2019) 291–301, https://doi.org/10.1016/j.compositesb.2018.12.083.

[21] Ye Li, En-Hua Yang, Kang Hai Tan, Flexural behavior of ultra-high performance hybrid fiber reinforced concrete at the ambient and elevated temperature, Constr. Build. Mater. 250 (2020) 118487, https://doi.org/10.1016/j.conbuildmat.2020.118487.

[22] J. Kim, G.-P. Lee, D.Y. Moon, Evaluation of mechanical properties of steel-fibre-reinforced concrete exposed to high temperatures by double-punch test, Constr. Build. Mater. 79 (2015) 182–191, https://doi.org/10.1016/j.conbuildmat.2015.01.042.

[23] D. Choumanidis, E. Badogiannis, P. Nomikos, A. Sofianos, Barcelona test for the evaluation of the mechanical properties of single and hybrid FRC, exposed to elevated temperature, Constr. Build. Mater. 138 (2017) 296–305, https://doi.org/10.1016/j.conbuildmat.2017.01.115.

[24] D.A.S. Rambo, A. Blanco, A.D. de Figueiredo, E.R.F. dos Santos, R.D. Toledo, O. da F.M. Gomes, Study of temperature effect on macro-synthetic fiber reinforced concretes by means of Barcelona tests: an approach focused on tunnels assessment, Constr. Build. Mater. 158 (2018) 443–453. https://doi.org/10.1016/j.conbuildmat.2017.10.046.

[25] Ramoel Serafini, Ronney R. Agra, Renan P. Salvador, Albert de la Fuente, Antonio D. de Figueiredo, Double edge wedge splitting test to characterize the design postcracking parameters of fiber-reinforced concrete subjected to high temperatures, J. Mater. Civ. Eng. 33 (5) (2021) 04021069, https://doi.org/10.1061/(ASCE)MT.1943-5533.0003701.

[26] Marco di Prisco, Liberato Ferrara, Marco G.L. Lamperti, Double edge wedge splitting (DEWS): an indirect tension test to identify post-cracking behaviour of fibre reinforced cementitious composites, Mater. Struct. 46 (11) (2013) 1893–1918, https://doi.org/10.1617/s11527-013-0028-2.

[27] A. Bentur, S. Mindess, Fibre Reinforced Cementitious Composites, 2nd ed., Taylor & Francis, United Kingdom, 2007.

[28] Albert de la Fuente, Pablo Pujadas, Ana Blanco, Antonio Aguado, Experiences in Barcelona with the use of fibres in segmental linings, Tunn. Undergr. Sp. Technol. 27 (1) (2012) 60–71, https://doi.org/10.1016/j.tust.2011.07.001.

[29] Brazilian National Standards Organization, ABNT NBR NM 67: Concrete - Slump test for determination of the consistency, 1998.

[30] L.A.C. Borges, R. Monte, D.A.S. Rambo, A.D. de Figueiredo, Evaluation of post-cracking behavior of fiber reinforced concrete using indirect tension test, Constr. Build. Mater. 204 (2019) 510–519, https://doi.org/10.1016/j.conbuildmat.2019.01.158.

[31] BS EN 1992-1-2, Eurocode 2 Design of concrete structures - Part 1-2: General rules - Structural fire design, 2004.

[32] The National Research Council of Italy (CNR), CNR-DT 204/2006, Guide for the Design and Construction of Fibre-Reinforced Concrete Structures, Rome, 2007. https://doi.org/10.14359/10516.
[33] J.M. Carpio, R. Serafini, D. Rambo, A. De La Fuente, A.D. De Figueiredo, Assessment of the bearing capacity reduction of FRC elements subjected to fire, in: Proc. Fib Symp. 2019 Concr. - Innov. Mater. Des. Struct., 2019.
[34] Ramoel Serafini, Ronney Rodrigues Agra, Luís A.G. Bitencourt, Albert de la Fuente, Antonio D. de Figueiredo, Bond-slip response of steel fibers after exposure to elevated temperatures: experimental program and design-oriented constitutive equation, Compos. Struct. 255 (2021) 112916, https://doi.org/10.1016/j.compstruct.2020.112916.
[35] Ulrich Schneider, Concrete at high temperatures — a general review, Fire Saf. J. 13 (1) (1988) 55–68, https://doi.org/10.1016/0379-7112(88)90033-1.
[36] Brazilian National Standards Organization, ABNT NBR 7215: Portland cement - Determination of compressive strength of cylindrical test specimens, 2019.
[37] Brazilian National Standards Organization, ABNT NBR 8522: Concrete - Determination of static modulus of elasticity and deformation by compression, 2017.
[38] W. de O. Bussab, P.A. Morettin, Estatística básica, São Paulo, 2010.
[39] H. Abuluwefa, R.I.L. Guthrie, F. Ajersch, The effect of oxygen concentration on the oxidation of low-carbon steel in the temperature range 1000 to 1250 °C, Oxid. Met. 46 (5-6) (1996) 423–440, https://doi.org/10.1007/BF01048639.
[40] R. Serafini, L.M. Mendes, R.P. Salvador, A.D. de Figueiredo, The effect of elevated temperatures on the properties of cold-drawn steel fibers, Mag. Concr. Res. (2020) 1–28, https://doi.org/10.1680/jmacr.19.00498.
[41] R.Y. Chen, W.Y.D. Yuen, Review of the high-temperature oxidation of iron and carbon steels in air or oxygen, Oxid. Met. (2003), https://doi.org/10.1023/A:1023685905159.
[42] J. Eidan, I. Rasoolan, A. Rezaeian, D. Poorveis, Residual mechanical properties of polypropylene fiber-reinforced concrete after heating, Constr. Build. Mater. 198 (2019) 195–206, https://doi.org/10.1016/j.conbuildmat.2018.11.209.
[43] Z.P. Bažant, M. Kaplan, Concrete at high temperatures: material properties and mathematical models, Longman, 1996.
[44] E. Gallucci, X. Zhang, K.L. Scrivener, Effect of temperature on the microstructure of calcium silicate hydrate (C-S-H), Cem. Concr. Res. 53 (2013) 185–195, https://doi.org/10.1016/j.cemconres.2013.06.008.
[45] Y.N. Chan, X. Luo, W. Sun, Compressive strength and pore structure of high-performance concrete after exposure to high temperature up to 800°C, Cem. Concr. Res. 30 (2) (2000) 247–251, https://doi.org/10.1016/S0008-8846(99)00240-9.
[46] R. Felicetti, P.G. Gambarova, G.A. Khoury, M.P. Natali-Sora, Mechanical Behaviour of HPC and UHPC in Direct Tension at High Temperature and after Cooling, in: 5th RILEM Symp. BEFIB'2020, RILEM Publ. S.A.R.L, Lyon (France), 2000: pp. 749–758.
[47] L.T. Phan, N.J. Carino, Effects of Test Conditions and Mixture Proportions on Behavior of High-Strength Concrete Exposed to High Temperatures, ACI Mater. J. 99 (2002), https://doi.org/10.14359/11317.
[48] N. Yermak, P. Pliya, A.-L. Beaucour, A. Simon, A. Noumowé, Influence of steel and/or polypropylene fibres on the behaviour of concrete at high temperature: Spalling, transfer and mechanical properties, Constr. Build. Mater. 132 (2017) 240–250, https://doi.org/10.1016/j.conbuildmat.2016.11.120.
[49] C.S. Poon, Z.H. Shui, L. Lam, Compressive behavior of fiber reinforced high-performance concrete subjected to elevated temperatures, Cem. Concr. Res. 34 (12) (2004) 2215–2222, https://doi.org/10.1016/j.cemconres.2004.02.011.
[50] Yuh-Shiou Tai, Huang-Hsing Pan, Ying-Nien Kung, Mechanical properties of steel fiber reinforced reactive powder concrete following exposure to high temperature reaching 800°C, Nucl. Eng. Des. 241 (7) (2011) 2416–2424, https://doi.org/10.1016/j.nucengdes.2011.04.008.
[51] Bing Chen, Juanyu Liu, Residual strength of hybrid-fiber-reinforced high-strength concrete after exposure to high temperatures, Cem. Concr. Res. 34 (6) (2004) 1065–1069, https://doi.org/10.1016/j.cemconres.2003.11.010.
[52] W. Zheng, H. Li, Y. Wang, Compressive stress–strain relationship of steel fiber-reinforced reactive powder concrete after exposure to elevated temperatures, Constr. Build. Mater. 35 (2012) 931–940, https://doi.org/10.1016/j.conbuildmat.2012.05.031.
[53] A. Bentur, S. Mindess, Fibre reinforced cementitious composites, CRC Press (2006), https://doi.org/10.1201/9781482267747.
[54] K.L. Scrivener, R. Snellings, B. Lothenbach, A Practical Guide to Microstructural Analysis of Cementitious Materials, CRC Press, Taylor & Francis Group, 2016.
[55] H. Taylor, Cement Chemistry, Thomas Telford, 2nd ed., Thomas Telford Publishing, London, 1997.
[56] Q. Ma, R. Guo, Z. Zhao, Z. Lin, K. He, Mechanical properties of concrete at high temperature—a review, Constr. Build. Mater. 93 (2015) 371–383, https://doi.org/10.1016/j.conbuildmat.2015.05.131.
[57] J. Li, J. Niu, C. Wan, X. Liu, Z. Jin, Comparison of flexural property between high performance polypropylene fiber reinforced lightweight aggregate concrete and steel fiber reinforced lightweight aggregate concrete, Constr. Build. Mater. 157 (2017) 729–736, https://doi.org/10.1016/j.conbuildmat.2017.09.149.
[58] J.-H. Lee, Influence of concrete strength combined with fiber content in the residual flexural strengths of fiber reinforced concrete, Compos. Struct. 168 (2017) 216–225, https://doi.org/10.1016/j.compstruct.2017.01.052.
[59] P. Pliya, A-L. Beaucour, A. Noumowé, Contribution of cocktail of polypropylene and steel fibres in improving the behaviour of high strength concrete subjected to high temperature, Constr. Build. Mater. 25 (4) (2011) 1926–1934, https://doi.org/10.1016/j.conbuildmat.2010.11.064.
[60] M. Di Prisco, G. Plizzari, L. Vandewalle, Fiber reinforced concrete in the new fib model code, in: 3rd Int. Fib Congr. Exhib. Inc. PCI Annu. Conv. Bridg. Conf. Think Glob. Build Locally, Proc., 2010.
[61] S. Abdallah, M. Fan, D.W.A. Rees, Effect of elevated temperature on pull-out behaviour of 4DH/5DH hooked end steel fibres, Compos. Struct. 165 (2017) 180–191, https://doi.org/10.1016/j.compstruct.2017.01.005.
[62] S. Abdallah, M. Fan, K.A. Cashell, Pull-out behaviour of straight and hooked-end steel fibres under elevated temperatures, Cem. Concr. Res. 95 (2017) 132–140, https://doi.org/10.1016/j.cemconres.2017.02.010.
[63] G. Ruano, F. Isla, B. Luccioni, R. Zerbino, G. Giaccio, Steel fibers pull-out after exposure to high temperatures and its contribution to the residual mechanical behavior of high strength concrete, Constr. Build. Mater. 163 (2018) 571–585, https://doi.org/10.1016/j.conbuildmat.2017.12.129.
[64] F.B. Varona, F.J. Baeza, D. Bru, S. Ivorra, Influence of high temperature on the mechanical properties of hybrid fibre reinforced normal and high strength concrete, Constr. Build. Mater. 159 (2018) 73–82, https://doi.org/10.1016/j.conbuildmat.2017.10.129.
[65] D. Choumanidis, E. Badogiannis, P. Nomikos, A. Sofianos, The effect of different fibres on the flexural behaviour of concrete exposed to normal and elevated temperatures, Constr. Build. Mater. 129 (2016) 266–277, https://doi.org/10.1016/j.conbuildmat.2016.10.089.
[66] M. Colombo, M. di Prisco, R. Felicetti, SFRC exposed to high temperature: Hot vs. residual characterization for thin walled elements, Cem. Concr. Compos. 58 (2015) 81–94, https://doi.org/10.1016/j.cemconcomp.2015.01.002.
[67] Sofren Leo Suhaendi, Takashi Horiguchi, Effect of short fibers on residual permeability and mechanical properties of hybrid fibre reinforced high strength concrete after heat exposition, Cem. Concr. Res. 36 (9) (2006) 1672–1678, https://doi.org/10.1016/j.cemconres.2006.05.006.